Study of the reaction $\bar{p}n \to \bar{p}p\pi^-$ at 14.6 GeV/c*

E. B. Brucker, E. L. Koller, O. Raths,† and S. Taylor
Stevens Institute of Technology, Hoboken, New Jersey 07030

P. E. Stamer
Seton Hall University, South Orange, New Jersey 07079

T. Handler, R. J. Plano, H. Preissner, and T. L. Watts
Rutgers—The State University, New Brunswick, New Jersey 08903

J. U. Grauman
Jersey City State College, Jersey City, New Jersey 07305

A. Fridman, J.-P. Gerber, M. E. Michalon-Mentzer, R. Schiby, and C. Voltolini
Centre de Recherches Nucléaires, Strasbourg, France
(Received 27 March 1974)

From a 98 000-photograph exposure of the BNL 80-in. deuterium-filled chamber to a 14.6-GeV/c $\bar{p}$ beam we have extracted those events that fit the channel $\bar{p}n \to \bar{p}p\pi^-$. The cross section for this channel is measured to be 730 ± 50 μb. The cross section for the reaction $\bar{p}n \to \bar{\Delta}^{--}(1238)p$ is determined to be 130 ± 30 μb. Evidence for target dissociation is presented. A comparison with the reaction $\pi^-n \to \pi^-p\pi^-$ at the same energy indicates agreement with factorization.

I. INTRODUCTION

We discuss here an analysis of the reaction $\bar{p}n \to \bar{p}p\pi^-$ at an incident momentum of 14.6 GeV/c. The data for this presentation have been extracted from a 98 000-picture exposure of the BNL 80-in. deuterium-filled bubble chamber to an rf-separated beam of antiprotons.

In Sec. II, we present the experimental procedure leading to the calculation of the cross section for $\bar{p}n \to \bar{p}p\pi^-$. The general features of this final state are given in Sec. III along with the cross section for the subchannel $\bar{\Delta}^{--}p$. These cross sections are then compared to those obtained for the same reactions but at lower incident beam momenta.

Aspects of target dissociation are discussed in Sec. IV. The similarities between these results and π^-n interactions at 15 GeV/c and pp interactions at 11.6 GeV/c are examined as a test of factorization. The data were tested also for compatability with either s- or t-channel helicity conservation.

II. EXPERIMENTAL PROCEDURE AND CROSS SECTIONS

The data for this report were obtained from a sample of four-pronged events where one of the outgoing positive prongs was heavily ionizing and consistent with stopping within the chamber. All of the film was scanned twice and the separate scans adjudicated and combined before measuring. A total of 6814 events were found.[1] The results of the first measuring pass were compared with the film and a remeasurement list was generated for those events which were not reconstructed, were poorly measured, or were not measured initially. Roughly 10% of the events were deemed unmeasurable because of obscured vertices, close-in scatters, etc. After remeasurement, approximately 95% of the events deemed measurable were reconstructed. In addition, a small sample of events (~300) were remeasured independent of their initial measuring status in order to check on the assignment of measuring errors. These two sets of measurements, and their subsequent kinematic fits, were identical within the assigned errors.

A total of 218 events were judged to be consistent with the selection criteria for the 4C (4-constraint) hypothesis

$$\bar{p}d \to p_s \bar{p}p\pi^- \ , \tag{1}$$

i.e., the observed spectator proton, p_s, had its momentum within the range 80 to 320 MeV/c, the track ionizations as determined by the fitted momenta were adjudged to be consistent with the film, and the χ^2 probability for the fit was greater than 1%. In no case was there an ambiguity between this reaction and other competing 4C channels. However, for about 10% of the events there was a track permutation ambiguity between the $\bar{p}$ and the π^-. For these cases only the higher probabil-

ity fit was retained.[2] For those events where the 4C hypothesis was satisfied as well as some other 1C hypothesis, the 4C hypothesis was retained since it was deemed to be the more reliable fit.

In Fig. 1(a) we display the momentum distribution of all protons from reaction (1). The momentum distribution of the slower proton (events not cross-hatched) is consistent with the Hulthén distribution (solid curve). The angular distribution between the slower proton and the beam direction, Fig. 1(b), shows evidence for a small depletion due to a systematic loss when the spectator proton is going backward to the beam but, otherwise, is isotropic. Therefore, we have assigned the slower proton to be the spectator even though approximately 20% of the events had both protons with momenta less than 320 MeV/c.

Accounting for the scanning and measuring losses as well as the selection criteria used, we determine the cross section for reaction (1) with two visible protons to be $225 \pm 15 \mu$b. Correcting for the invisible spectator protons by using the Fourier transform of the Hulthén wave function[3] yields a cross section of 670 ± 45 μb. Finally, applying a correction for Glauber screening[4] yields the cross section for the reaction

$$\bar{p}n \to \bar{p}p\pi^- \tag{2}$$

of 730 ± 50 μb.

The comparison of the cross section found in this experiment with the cross sections for the same reaction as obtained at 3.5, 5.5, and 7.0 GeV/c (see Refs. 5, 6, and 7, respectively) incident momenta is displayed in Fig. 2 as the upper set (a) of data points. A fit of these data to the form $\sigma = A p_{\text{lab}}^{-b}$ yields a value of $b = 0.97 \pm 0.07$ which is displayed as the solid line.

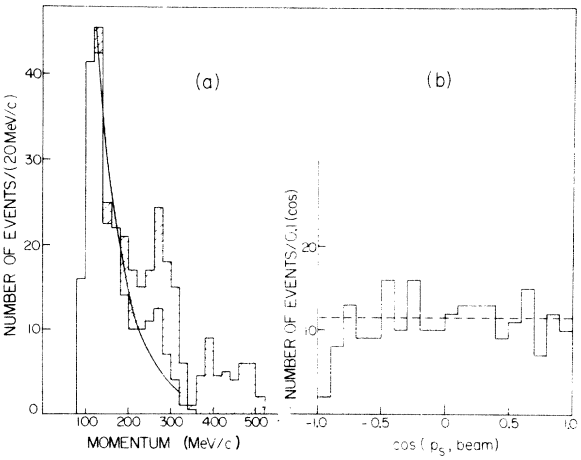

FIG. 1. (a) Distribution of the laboratory momentum of the two protons from reaction (1). The faster proton is denoted by the cross-hatched area. The solid curve is the Hulthén momentum spectrum normalized to the number of events in the range 120 to 280 MeV/c. (b) Distribution of the cosine of the angle between the spectator proton and the beam direction. The dashed curve represents the average number of events per interval for $\cos(p_s, \text{beam}) > -0.8$.

III. GENERAL FEATURES

In Fig. 3 we display the three-body Van Hove plot.[8] The peripheral character of the reaction is evident in that the $\bar{p}$ is forward in the center of momentum and near the kinematic momentum limit. The outgoing proton is fast and backward while the π^- is, in general, slow and more isotropically distributed. Of the few backward $\bar{p}$ events, most correspond to an ambiguous identification of the $\bar{p}$ and π^-.

The histograms for the four-momentum transfer squared as calculated from the initial- and final-state antiproton, $|t_{\bar{p}}|$, and from the initial neutron and final proton, $|t_n|$, are shown in Fig. 4. The histogram for the $\bar{p}$ vertex shows a clear exponential form but with an apparent change of slope at $|t_{\bar{p}}| \approx 0.2$ (GeV/c)^2. The interval $0 \leq |t_{\bar{p}}| < 0.2$ (GeV/c)^2 has a slope, b, of 8.4 ± 1.5 (GeV/c)$^{-2}$ when fitted to the form $e^{-b|t_{\bar{p}}|}$. This fit is also shown in Fig. 4(a). No attempt was made to fit the high-t data. The histogram for the nucleon vertex has an obviously different t dependence.

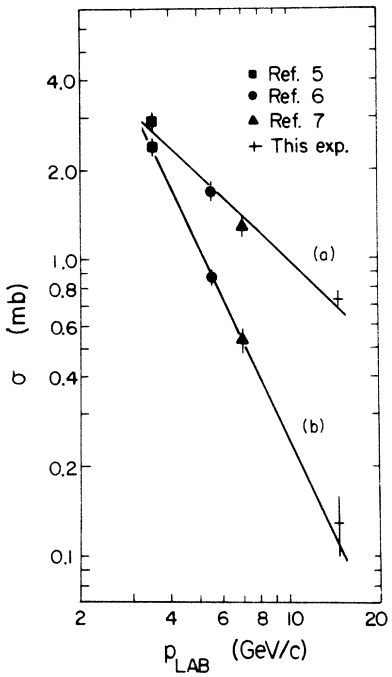

FIG. 2. The cross sections for (a) $\bar{p}n \to \bar{p}p\pi^-$ and (b) $\bar{p}n \to \bar{\Delta}^{--}p$ as determined at laboratory momentum 3.5, 5.5, 7.0, and 14.6 GeV/c. The solid curves are defined in Secs. II and III.

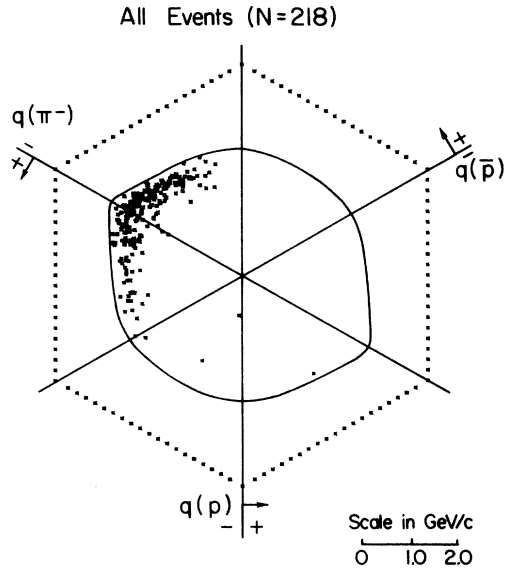

FIG. 3. Van Hove plot, where $q(p)$, $q(\bar{p})$, and $q(\pi^-)$ are the longitudinal momenta of the p, $\bar{p}$, and π^- in the $\bar{p}n$ center-of-mass system. The solid curve is the kinematic boundary.

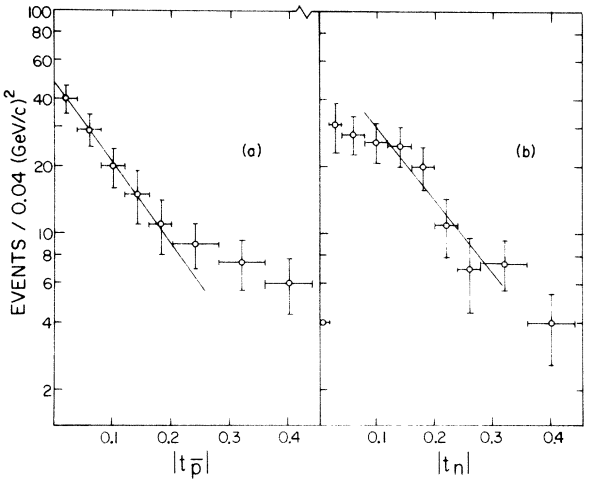

FIG. 4. Histograms of four-momentum transfer squared for (a) the $\bar{p}$ vertex and (b) the nucleon vertex in units of $(\mathrm{GeV}/c)^2$. The curves are the best fit over the intervals shown, as described in the text.

The fit to the exponential form has a slope of 7.5 ± 2.0 $(\mathrm{GeV}/c)^{-2}$ for the interval $0.1 \leq |t_n| < 0.3$ $(\mathrm{GeV}/c)^2$. These results are similar to the t dependence for the reaction $pn \to pp\pi^-$ at 11.6 GeV/c as measured by the Weizmann group.[9] A comparison of the slopes of the t-distributions for these two experiments is a part of Table I.

The Dalitz plot of the mass-squared distribution $M^2(p\pi^-)$ vs $M^2(\bar{p}\pi^-)$ is displayed in Fig. 5. The boundary of this plot is calculated for an incident $\bar{p}$ interacting with a free neutron assumed to be at rest. The Fermi motion of the target allows a few events to fall outside of this boundary. A noteworthy feature of the plot is the relative lack of events in the region of simultaneous low $M(p\pi^-)$ and the $\bar{\Delta}^{--}$ (1238) (see below).

The histograms of the three possible effective-mass combinations are shown in Fig. 6. In Fig. 6(a) is the effective-mass histogram of the $p\pi^-$ system, $M(p\pi^-)$, for all events and for those events where the π^- is backward in the c.m. frame $(\cos\theta^*_\pi \leq 0.0)$. There is no evidence for the dominance of an N^* formation. However, there is a broad low-mass enhancement which is associated with the backward going π^-. This spectrum is fairly well reproduced by a Monte Carlo phase space that has been modified to reflect the observed t distributions, $t_{\bar{p}}$ and t_n (dashed curve). The fraction of events with $M(p\pi^-) < 1.75$ GeV/c^2 in this experiment is greater than the fraction observed in the same reaction at either 5.5 or 7.0 GeV/c. Further comment about this low-mass region is deferred until Sec. IV.

TABLE I. A comparison of the slopes of the four-momentum-transfer distributions for $\bar{p}n \to \bar{p}p\pi^-$, $\pi^-n \to \pi_f^- p \pi_s^-$ (Ref. 14) and $pn \to pp\pi^-$ (Ref. 9). t_B is the four-momentum transferred to the beam particle; t_n is for the target nucleon. For t'_B see Sec. IV.

Reaction	t_B Interval $[(\mathrm{GeV}/c)^2]$	t_B Slope $[(\mathrm{GeV}/c)^{-2}]$	t_n Interval $[(\mathrm{GeV}/c)^2]$	t_n Slope $[(\mathrm{GeV}/c)^{-2}]$	t'_B Interval $[(\mathrm{GeV}/c)^2]$	t'_B Slope $[(\mathrm{GeV}/c)^{-2}]$
$\bar{p}n \to \bar{p}p\pi^-$	$0 \leq \lvert t\rvert \leq 0.2$	8.4 ± 1.5	$0.1 \leq \lvert t\rvert \leq 0.3$	7.5 ± 2.0	$M(p\pi^-) < 1.4$ $0 \leq \lvert t'\rvert \leq 0.2$	15 ± 2
					$1.4 \leq M(p\pi^-) < 1.75$ $0 \leq \lvert t'\rvert \leq 0.4$	6 ± 2
$pn \to p_b p_n \pi^-$	$0 \leq \lvert t\rvert \leq 0.4$	9.1	$0.18 \leq \lvert t\rvert \leq 0.4$	9.5	...	...
$\pi^-n \to \pi_f^- p \pi_s^-$	...	...	...	...	$M(p\pi_s^-) < 1.4$ $0 \leq \lvert t'\rvert \leq 0.2$	15
					$1.4 \leq M(p\pi_s^-) < 2.0$ $0 < \lvert t'\rvert \leq 0.4$	5.7

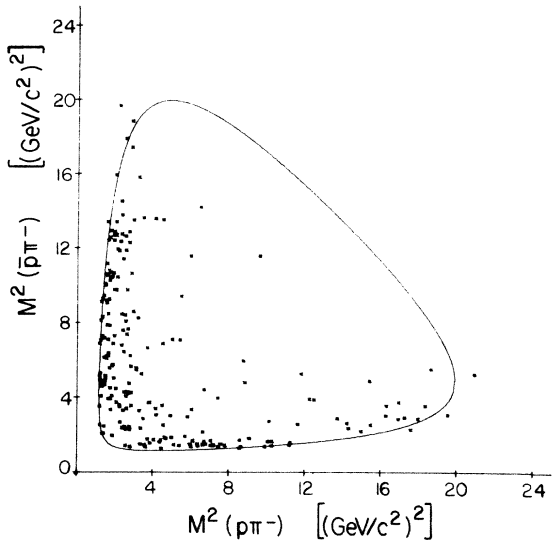

FIG. 5. Dalitz plot of $M^2(p\pi^-)$ vs $M^2(\bar{p}\pi^-)$. The boundary is defined in Sec. III.

The histogram of the effective mass of the $\bar{p}\pi^-$ system, $M(\bar{p}\pi^-)$, is shown in Fig. 6(b) for all events and for those events where the π^- is now forward in the c.m. frame. There is an excess of events in the region of $\bar{\Delta}^{--}$ (1238) associated entirely with the forward-going π^-. This means that there is no overlap between the $\bar{\Delta}$ signal and the events with low $M(p\pi^-)$. Using these events we estimate a $\bar{\Delta}$ cross section above background for the reaction

$$\bar{p}n \to \bar{\Delta}^{--}p \tag{3}$$

of 130 ± 30 μb. The comparison of this result with cross sections for the same reaction at the lower momenta is displayed in Fig. 2 as the lower set (b) of data points. Again assuming an energy dependence of the form $\sigma = Ap_{\text{lab}}^{-b}$ we derive $b = 2.13 \pm 0.14$ as shown.

Although the $\bar{p}p$ effective-mass spectrum in Fig. 6(c) appears to contain some sort of structure, the apparent peaks are associated with the low-mass structure in the $p\pi^-$ and $\bar{p}\pi^-$ spectra.

IV. NEUTRON DIFFRACTION DISSOCIATION

It is natural to assume that the accumulation of events at low $M(p\pi^-)$ is a manifestation of diffraction of the target neutron as seen in other experiments.[10,11] Excluding $\bar{\Delta}$ (1238) production, the cross section for all other $\bar{p}n$ processes leading to a $\bar{p}p\pi^-$ final state appears to be relatively insensitive to the beam momentum from 3.5 to 14.6 GeV/c. (See Fig. 2.) This feature is a commonly accepted characteristic of diffraction dissociation.[10]

In addition, for this experiment we present in

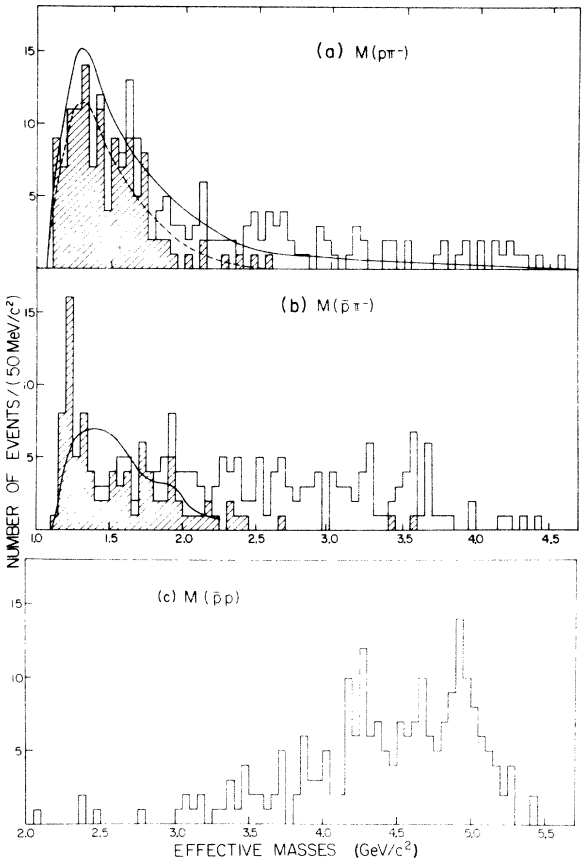

FIG. 6. Invariant-mass histograms. (a) Effective mass of the $p\pi^-$ system. The cross-hatched events correspond to the π^- in the backward hemisphere. The solid curve is a Monte Carlo prediction of phase space as discussed in Sec. III. The dashed curve is the same Monte Carlo prediction but selected on a backward π^-. (b) Effective mass of $\bar{p}\pi^-$. The shaded events are for a forward-going π^-. The solid curve is the Monte Carlo prediction selected on the forward pion. (c) The effective mass of the $\bar{p}p$ system.

Fig. 7 histograms of $|t'_{\bar{p}}|$, where $t'_{\bar{p}} = t_{\bar{p}} - t_{\min}$ for two mass intervals: (a) $M(p\pi^-) < 1.4$ GeV/c^2 and (b) $1.4 \leq M(p\pi^-) < 1.75$ GeV/c^2. When fitted to the form $e^{-b'|t'_{\bar{p}}|}$ these histograms have slopes, b', of 15 ± 2 and 6 ± 2 (GeV/c)$^{-2}$, respectively (see also Table I). At a fixed s, the square of the c.m. energy, this correlation of b' with the mass of a diffractively produced system has been predicted by Satz[12] and Dorren *et al.*[13]

Recently a Seattle-Berkeley collaboration has reported[14] on the reaction

$$\pi^-n \to \pi_f^- p \pi_s^- \tag{4}$$

at 15 GeV/c, where π_f^- and π_s^- denote the faster or slower π^-, respectively. They observe the same t' dependence for the corresponding mass regions;

see Table I.

If the observed effects are indeed due to diffraction dissociation of the target neutron then we can test factorization of an "effective" trajectory with vacuum quantum numbers by comparing the invariant cross section

$$s\frac{d^2\sigma}{dtdM^2}$$

for reaction (2) and reaction (4) with $d\sigma_{el}/dt\,(\bar{p}n)$ and $d\sigma_{el}/dt\,(\pi^-n)$, respectively. However, s for Ref. 14 is within 2% of the value of this experiment, the mass intervals are identical and the slopes of the corresponding t' distributions are equal, within errors. Therefore we can compare the ratio

$$R=\frac{\sigma^*}{\sigma_{el}} \tag{5}$$

for the two experiments, where σ^* is the cross section,[15] integrated over all t', for events with $M(p\pi^-)< 1.4$ GeV/c^2. Since neither $\sigma_{el}(\pi^-n)$ nor $\sigma_{el}(\bar{p}n)$ has been measured at these energies, we use $\sigma_{el}(\bar{p}p)$ (see Ref. 16) for $\sigma_{el}(\bar{p}n)$ and use the elastic cross section for the charge-conjugate reaction π^+p (Ref. 17) in place of $\sigma_{el}(\pi^-n)$. Because of the uncertainties introduced by the replacement of the $\bar{p}n$ cross section by the $\bar{p}p$ cross section we have also computed the ratio

$$R'=\frac{\sigma^*}{\sigma_{tot}}\,, \tag{6}$$

where $\sigma_{tot}\,(\bar{p}n)$ has been measured.[18] These ratios, R and R', are the same within errors for the two experiments; see Table II.

TABLE II. Comparison of the reactions $\bar{p}n \to \bar{p}p\pi^-$ and $\pi^-n \to \pi^-p\pi^-$.

	π^-n	$\bar{p}n$
σ (μb)	310 ± 3^a	730 ± 50
σ^* (μb)	95 ± 6	200 ± 26
σ_{el} (mb)	4.46 ± 0.15^b	9.0 ± 0.6^c
σ_{tot} (mb)	24.10 ± 0.08^b	53.2 ± 3.7^d
$R=\sigma^*/\sigma_{el}$	$(2.13\pm0.15)\times10^{-2}$	$(2.22\pm0.32)\times10^{-2}$
$R'=\sigma^*/\sigma_{tot}$	$(3.94\pm0.25)\times10^{-3}$	$(3.76\pm0.55)\times10^{-3}$

[a] π^+p : Ref. 15.
[b] π^+p : Ref. 17.
[c] $\bar{p}p$: Ref. 16.
[d] $\bar{p}n$: Ref. 18.

Finally, for diffractive processes, it has been conjectured that helicity may be conserved in either the s or t channel.[19] Irrespective of a definite spin assignment of a diffractively produced system, the azimuthal distribution $\bar{\phi}_{G-J}$ $(\bar{\phi}_H)$ of the π^- should be isotropic in the Gottfried-Jackson (helicity) frame if there is t- (s-) channel helicity conservation.[20] These azimuthal distributions[21] are displayed in Fig. 8. Apart from a reduction in the size of the data sample, there is no qualitative difference in these distributions between the entire sample and those events with low $M(p\pi^-)$. Within the limited statistics definite statements about helicity conservation are impossible.

V. CONCLUSIONS

At the energy of this experiment we have shown that the quasi-two-body production $\bar{p}n \to \bar{\Delta}^{--}p$ is

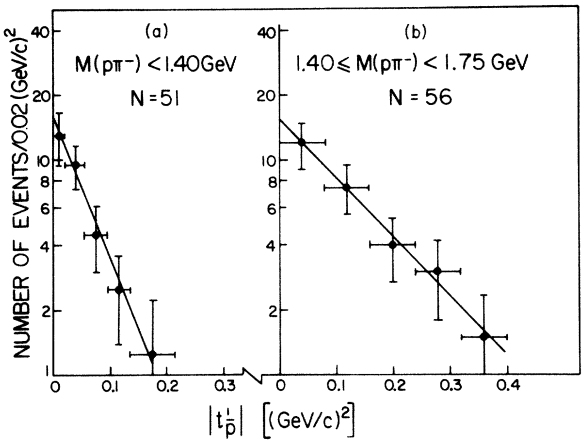

FIG. 7. Histograms of four-momentum transferred for the $\bar{p}$ vertex when $M(p\pi^-)$ is (a) less than 1.4 GeV and (b) between 1.4 and 1.75 GeV. The straight lines are the best fits as described in the text.

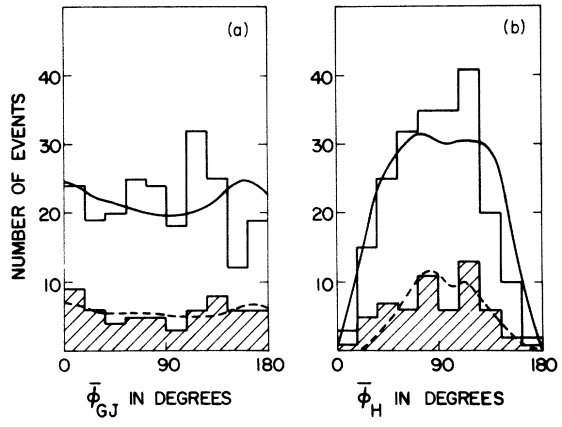

FIG. 8. Azimuthal distributions in the (a) Gottfried-Jackson $(\bar{\phi}_{G-J})$ and (b) helicity $(\bar{\phi}_H)$ frames of the $p\pi^-$. The cross-hatched events satisfy $M(p\pi^-)$ <1.4 GeV. The curves are the Monte Carlo predictions for all events and for those events with $M(p\pi^-)$ <1.4 GeV.

a small fraction of the interaction cross section. The dominant feature of the data appears to be target dissociation which is separable from the $\bar{\Lambda}$ production. We have demonstrated a similarity of the dissociation of the neutron in reaction (2) and (4). In the context of Regge models, we believe we have demonstrated agreement with factorization to the 15% level. We note that this test is performed for $t \neq 0$ as compared with those tests at $t = 0$ from inclusive reactions.[22] On the other hand, without at least a knowledge of the s dependence, we cannot identify the particular trajectory exchanged.

ACKNOWLEDGMENTS

We wish to acknowledge the cooperation of the staffs of the AGS and the 80-in. bubble chamber in obtaining this exposure. The diligent efforts of the staff at Stevens, Rutgers, and Strasbourg in scanning and measuring the film is appreciated. We would like to thank Dr. W. C. Harrison of Rutgers for the use of his Monte Carlo programs. Finally, we are especially indebted to Professor T. F. Wong and Professor J. Bronzan for stimulating and enlightening discussions on the question of factorization.

---

*Work supported in part by the National Science Foundation and the U. S. Office of Naval Research.

†Work submitted in partial fulfillment of requirements for the degree of Doctor of Philosophy at Stevens Institute of Technology. Present address: Wagner College, Staten Island, New York 10301.

[1]The film was divided equally between the Strasbourg group and the Rutgers-Stevens group. All scanning, measuring, and event selection were performed independently by the two groups. There appear to be no systematic differences between the two sets of data and, hence, only the combined results are presented. However, the cross section for the reaction $\bar{p}n \to \bar{p}p\pi^-$ was computed independently by each group and a weighted average is presented.

[2]All histograms were also reproduced giving one-half weight to each of these possible permutations. No significant differences were seen.

[3]For a discussion of this correction see, for example, R. Kraemer *et al.*, Phys. Rev. 136, B496 (1964).

[4]V. Franco and R. J. Glauber, Phys. Rev. 142, 1195 (1966). For a discussion of this correction as applied to Reaction 1 see also Ref. 6.

[5]D. A. Huwe, Ohio University (private communication).

[6]H. Braun *et al.*, Phys. Rev. D 2, 488 (1970).

[7]P. Antich *et al.*, Nucl. Phys. B43, 45 (1972).

[8]L. Van Hove, Nucl. Phys. B9, 331 (1969).

[9]D. Hochman *et al.*, Weizmann Institute Report No. WIS 73/25 Ph (unpublished).

[10]For a comprehensive review of the experimental results on diffractive processes see, for instance, D. W. G. S. Leith, SLAC Report No. SLAC-Pub-1330, 1973 (unpublished) and the supplement to SLAC-Pub-1330, 1973 (unpublished).

[11]J. Ballam *et al.*, Phys. Rev. D 4, 1946 (1971).

[12]H. Satz, Phys. Lett. 32B, 380 (1970).

[13]D. Dorren, V. Rittenberg, and D. Yaffe, Nucl. Phys. B30, 306 (1971).

[14]P. L. Bastien *et al.*, University of Washington Report No. VTL Pub. (13) (unpublished).

[15]Since the results presented in Ref. 14 do not contain cross sections, we have scaled their results using the cross section for the charge-conjugate reaction $\pi^+p \to \pi^+n\pi^+$ at 15 GeV/c: ABBCCW Collaboration, CERN Report No. CERN/HERA 72-1 (unpublished).

[16]Extrapolated to 15 GeV/c using the values of K. J. Foley *et al.*, Phys. Rev. Lett. 11, 503 (1963).

[17]S. J. Lindenbaum *et al.*, Phys. Rev. Lett. 19, 330 (1967).

[18]W. Galbraith *et al.*, Phys. Rev. 138, B913 (1965).

[19]See, for instance, F. Gilman *et al.*, Phys. Lett. 31B, 387 (1970); J. V. Beaupré *et al.*, Nucl. Phys. B47, 51 (1972).

[20]G. Cohen-Tannoudji, J. M. Drouffe, P. Moussa, and R. Peschanski, Phys. Lett. 33B, 183 (1970).

[21]For a definition of these coordinate frames see, e.g., H. Braun *et al.*, Phys. Rev. D 8, 2765 (1973).

[22]See, for example, T. F. Wong, Phys. Rev. D 6, 2410 (1970); M. S. Chen *et al.*, Phys. Rev. Lett. 26, 1585 (1971).